

# Transport properties and magnetic field induced localization in the misfit cobaltite $[\text{Bi}_2\text{Ba}_{1.3}\text{K}_{0.6}\text{Co}_{0.1}]^{\text{RS}}[\text{CoO}_2]_{1.97}$ single crystal

X. G. Luo, H. Chen, G. Y. Wang, G. Wu, T. Wu, L. Zhao, and X. H. Chen\*

*Hefei National Laboratory for Physical Science at Microscale and Department of Physics, University of Science and Technology of China, Hefei, Anhui 230026, People's Republic of China*

Resistivity under magnetic field, thermopower and Hall coefficient are systematically studied for  $[\text{Bi}_2\text{Ba}_{1.3}\text{K}_{0.6}\text{Co}_{0.1}]^{\text{RS}}[\text{CoO}_2]_{1.97}$  single crystal. In-plane resistivity ( $\rho_{ab}(T)$ ) shows metallic behavior down to 2 K with a  $T^2$  dependence below 30 K; while out-of-plane resistivity ( $\rho_c(T)$ ) shows metallic behavior at high temperature and a thermal activation semiconducting behavior below about 12 K. Striking feature is that magnetic field induces a  $\ln(1/T)$  diverging behavior in both  $\rho_{ab}$  and  $\rho_c(T)$  at low temperature. The positive magnetoresistance (MR) could be well fitted by the formula based on multi-band electronic structure. The  $\ln(1/T)$  diverging behavior in  $\rho_{ab}$  and  $\rho_c(T)$  could arise from the magnetic-field-induced 2D weak localization or spin density wave.

PACS numbers: 75.30.-m, 71.30.+h, 71.70.-d, 75.47.-m

## I. INTRODUCTION

Triangular cobaltites have attracted significant interest for the promising application prospect as thermoelectrical materials and the complex physical properties as strongly correlated electron system.[1, 2, 3, 4] The complex physical properties include the unconventional superconductivity in water-intercalated  $\text{Na}_{0.35}\text{CoO}_2$ ,[5] temperature-dependent Hall effect,[3, 6] large negative MR in  $(\text{Bi,Pb})_2\text{M}_2\text{Co}_2\text{O}_y$  ( $M=\text{Sr}$  and  $\text{Ca}$ ) and  $\text{Ca}_3\text{Co}_4\text{O}_9$ ,[2, 6, 7] large thermopower (TEP) with low resistivity,[1, 2] and complicated magnetic structure,[8, 9, 10] etc. These triangular cobaltites have the common structural unit of  $\text{CdI}_2$ -type hexagonal  $[\text{CoO}_2]$  layer, which is composed of edge-shared  $\text{CoO}_6$  octahedra. Among them, the so-called misfit cobaltites  $\text{Bi}_2\text{M}_2\text{Co}_2\text{O}_y$  ( $M=\text{Ca}$ ,  $\text{Sr}$  and  $\text{Ba}$ ) [11] and  $\text{Ca}_3\text{Co}_4\text{O}_9$  [2] are constructed by the alternative stacking rocksalt(RS)-type blocks and  $[\text{CoO}_2]$  layers. The two sublattices share the common  $a$ - and  $c$ -lattice parameters, but possess the different  $b$ -lattice lengths causing a misfit along  $b$ -axis with a misfit ratio  $b_{\text{RS}}/b_{\text{H}}$  ( $b_{\text{RS}}$  and  $b_{\text{H}}$  are the  $b$ -lattice parameters for RS and hexagonal sublattices, respectively). In  $\text{Bi}_2\text{M}_2\text{Co}_2\text{O}_y$  ( $M=\text{Ca}$ ,  $\text{Sr}$  and  $\text{Ba}$ ), the quadruple RS block is composed of two deficient  $[\text{BiO}]$  layers sandwiched by two  $[\text{MO}]$  layers.[11] As  $M=\text{Ba}$ , commensurate modulation along  $b$ -axis between RS and hexagonal sublattices with  $b_{\text{RS}}/b_{\text{H}}=2.0$  was found,[12] being in contrast to the incommensurate modulation in other misfit cobaltites. Metallicity increases with increasing the ionic radii from  $\text{Ca}$  to  $\text{Ba}$ ,[6, 7, 12] and the MR at low temperature also changes the sign from negative in  $\text{Ca}$  and  $\text{Sr}$  compounds[6, 7] to positive in  $\text{Ba}$  compounds.[12] It has been found by us that there coexist large negative and positive contributions to the nonmonotonic magnetic-field dependent MR in  $\text{Pb}$ -doped  $\text{Bi}_2\text{Sr}_2\text{Co}_2\text{O}_y$ ,[13] Spin-dependent charge transport has been taken into account for understanding the large negative MR in  $\text{Sr}$  and  $\text{Ca}$  compounds, but the large positive MR in  $\text{Ba}$  compounds has not been fully understood. In

polycrystalline  $\text{Bi}_2\text{Ba}_2\text{Co}_2\text{O}_y$  sample, Hervieu et al. reported that the positive isothermal MR exhibits a linear  $H$  dependence. They compared the behavior in  $\text{Ba}$  compounds with MR in  $\text{Sr}_2\text{RuO}_4$  and heavy-Fermion-like oxide  $\text{LiV}_2\text{O}_4$  to understand the positive MR.[12] However, the origin of large positive MR was not settled down, further work, especially on single crystals, is required to understand this anomalous positive MR.

In this article,  $\text{K}$ -doped  $\text{Bi}_2\text{Ba}_2\text{Co}_2\text{O}_y$  single crystal was grown through flux method. The single crystal shows metallic resistivity in  $ab$  plane down to 2 K, while exhibits a weak thermal activation behavior along  $c$ -axis at low temperature. Magnetic field induces a  $\ln(1/T)$  diverging behavior at low temperature in  $\rho_{ab}(T)$  and  $\rho_c(T)$ . The positive MR can be interpreted by the multiband electronic structure. The  $\ln(1/T)$  diverging behavior in  $\rho_{ab}(T)$  may be ascribed to the magnetic-field-induced 2D weak localization or spin density wave (SDW).

## II. EXPERIMENTAL PROCEDURES

$\text{Bi-Ba-Co-O}$  single crystals were grown by the solution method using  $\text{K}_2\text{CO}_3\text{-KCl}$  fluxes. Starting materials  $\text{Bi}_2\text{O}_3$ ,  $\text{BaCO}_3$  and  $\text{Co}_3\text{O}_4$  were mixed in a proportion of  $\text{Bi}:\text{Ba}:\text{Co} = 2:2:2$  with a total weight to be 4 grams. The powders were heated at  $800^\circ\text{C}$  for 10 hours. Then the prepared  $\text{Bi}_2\text{Ba}_2\text{Co}_2\text{O}_y$  was mixed with the mixture of  $\text{KCl}$  and  $\text{K}_2\text{CO}_3$  with a molar proportion of 1:4 (20.5 grams), which was loaded in an aluminum crucible having 30 ml volume. The solute concentration was about 1.5 mol%. A lidded crucible was used to prevent the solution from evaporating and to grow crystals under stable conditions. The mixture was melted at  $950^\circ\text{C}$  for 20 hours, and then slowly cooled down to  $600^\circ\text{C}$  at a rate of  $5^\circ\text{C/hr}$ . The single crystals were separated from the melt by washing with distilled water. The crystals were large thin platelets and black in color. Typical dimensions of the crystals are  $5\times 5\times 0.05\text{ mm}^3$ .

Single crystals were characterized by electron diffrac-

tion (ED) and x-ray diffractions (XRD) using Cu  $K_\alpha$  radiations, respectively. The actual chemical composition of the single crystals was determined by inductively coupled plasma (ICP) atomic emission spectroscopy (AES) (ICP-AES) technique and X-ray Energy Dispersive Spectrum (EDS). The obtained results from ICP-AES and EDS were almost consistent to be Bi: Ba: K: Co = 2: 1.3: 0.6: 2.1.

Electrical transport was measured using the ac four-probe method with an alternative current (ac) resistance bridge system (Linear Research, Inc.; LR-700P). Hall effect is measured by four-terminal ac technique. To eliminate the offset voltage due to the asymmetric Hall terminals, the magnetic field was changed from -5 to 5 T and the Hall voltage was calculated to be  $\{V(H) - V(-H)\}/2$ , where  $V$  is the voltage between the Hall probes. The dc magnetic field for MR measurements is supplied by a superconducting magnet system (Oxford Instruments). Thermoelectric power (TEP) was measured using the steady-state technique.

### III. EXPERIMENTAL RESULTS

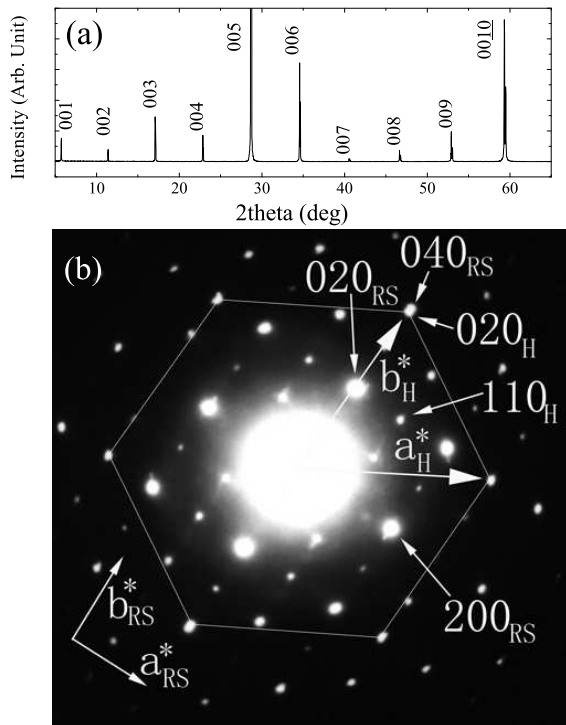


FIG. 1: (a):X-ray diffraction pattern; (b): [001] electron diffraction pattern for the  $[\text{Bi}_2\text{Ba}_{1.3}\text{K}_{0.6}\text{Co}_{0.1}]^{RS}[\text{CoO}_2]_{1.97}$  single crystal

#### A. Structural characterization

XRD pattern shown in Fig. 1a indicates that the single crystals are perfect c-orientation with the c-axis lattice parameter of 15.55 Å, larger than that in undoped polycrystalline sample (15.44 Å),[12] being consistent with the substitution of larger  $\text{K}^+$  for  $\text{Ba}^{2+}$  ion ( $r_{\text{K}^+} = 1.38$  Å,  $r_{\text{Ba}^{2+}} = 1.36$  Å).[14] The [001] ED pattern shown in Fig.1b is similar to that of undoped sample reported by Hervieu et al.[12] except for that the reflection of  $(020)_H$  visibly separates from that of  $(040)_{RS}$  (where H and RS refer to the hexagonal and RS sublattices, respectively). In-plane lattice parameters can be estimated from the [001] ED pattern.  $\mathbf{a}$  and  $\mathbf{b}$  parameter of RS sublattice is larger than those in undoped polycrystalline sample.  $a_{RS}$  and  $b_{RS}$  are 4.905 and 5.640 Å for undoped polycrystalline sample, while 5.031 and 5.683 Å for the present single crystal, respectively. This is due to the substitution of larger  $\text{K}^+$  for  $\text{Ba}^{2+}$  ion. Along  $\mathbf{a}$  axis, it is obtained  $a_{RS} = \sqrt{3}a_H$  ( $a_H = 2.907$  Å), indicating that the RS and H subsystems share the common a-axis lattice parameter. Along  $\mathbf{b}$  axis, however, an incommensurate modulation with the misfit ratio  $b_{RS}/b_H = 1.97$  ( $b_H = 2.88$  Å) can be obtained, indicating that  $\mathbf{b}_{RS}$  and  $\mathbf{b}_H$  axes are colinear but aperiodic. This is in contrast to the commensurate modulation along  $\mathbf{b}$  direction in undoped polycrystalline sample ( $b_{RS}/b_H = 2$ ).[12] Therefore, the structural formula of the present compound could be written as  $[\text{Bi}_2\text{Ba}_{1.3}\text{K}_{0.6}\text{Co}_{0.1}]^{RS}[\text{CoO}_2]_{1.97}$ .

#### B. Resistivity, Hall coefficient and thermopower

Figure 2a shows the temperature dependence of the in-plane and out-of-plane resistivity ( $\rho_{ab}(T)$  and  $\rho_c(T)$ ) for  $[\text{Bi}_2\text{Ba}_{1.3}\text{K}_{0.6}\text{Co}_{0.1}]^{RS}[\text{CoO}_2]_{1.97}$  single crystal.  $\rho_{ab}(T)$  shows metallic behavior down to 2 K. This contrasts to the semiconducting behavior below 80 K in the undoped polycrystalline sample.[12] It suggests that K doping on the Ba sites induces excess charge carriers into the system. Figure 2c indicates that the metallic in-plane resistivity below 30 K follows  $T^2$ -dependence, indicative of strong electron correlation in the crystal. Such behavior is similar to that observed in  $\text{Na}_{0.7}\text{CoO}_2$ . [4] However, out-of-plane resistivity shows a weak semiconducting behavior below 12 K. Figure 2d indicates that the weak semiconducting behavior obeys thermal activation behavior with an activation energy of 0.013 meV. At high temperature, the out-of-plane resistivity shows metallic behavior up to room temperature. No incoherent-to-coherent behavior is observed in this crystal, contrasting to the Pb-doped  $\text{Bi}_2\text{Ba}_2\text{Co}_2\text{O}_y$ , [15] in which  $\rho_{ab}(T)$  is metallic down to 2 K, while  $\rho_c(T)$  shows a incoherent-to-coherent transition at about 180 K with decreasing temperature. It should be pointed out that metallic behavior in  $\rho_{ab}(T)$  and semiconducting-like behavior in  $\rho_c(T)$  is similar to the case of underdoped sample in the high- $T_c$

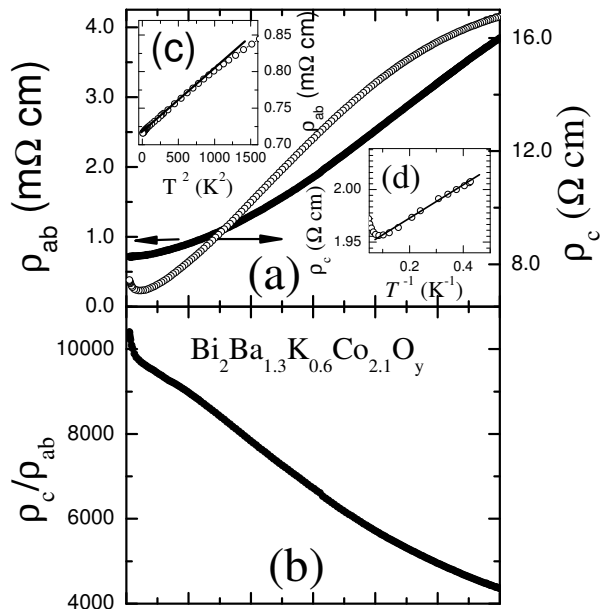


FIG. 2: (a): Temperature dependence of in-plane and out-of-plane resistivity; (b): Temperature dependence of resistivity anisotropy  $\rho_c/\rho_{ab}$  for the  $[\text{Bi}_2\text{Ba}_{1.3}\text{K}_{0.6}\text{Co}_{0.1}]^{RS}[\text{CoO}_2]_{1.97}$  single crystal. (c):  $T^2$  dependence of the in-plane resistivity below 50 K; (d): Plot of  $\ln(\rho_c)$  vs  $(1/T)$

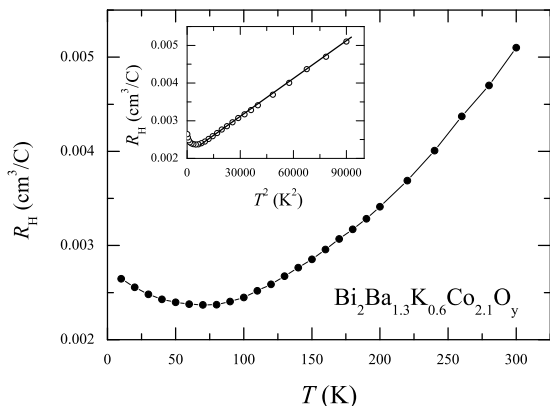


FIG. 3: Temperature dependence of the Hall coefficient for the  $[\text{Bi}_2\text{Ba}_{1.3}\text{K}_{0.6}\text{Co}_{0.1}]^{RS}[\text{CoO}_2]_{1.97}$  single crystal. Inset shows the square  $T$  dependence of the Hall coefficient.

cuprates, in which  $\rho_{ab}(T)$  shows metallic behavior, while  $\rho_c(T)$  becomes divergency at low temperature.[16] This behavior is ascribed to opening of pseudogap. However, similar behavior in  $[\text{Bi}_2\text{Ba}_{1.3}\text{K}_{0.6}\text{Co}_{0.1}]^{RS}[\text{CoO}_2]_{1.97}$  single crystal cannot be understood so far. Figure 2b shows the temperature dependence of anisotropy  $\rho_c/\rho_{ab}$ . The  $\rho_c/\rho_{ab}$  is larger than  $\sim 10^3$  in the whole temperature,

suggesting the highly anisotropic electronic structure. The anisotropy  $\rho_c/\rho_{ab}$  increases with decreasing temperature, similar to that observed in the  $(\text{Bi,Pb})_2\text{Sr}_2\text{Co}_2\text{O}_y$  crystals.[13] Strongly temperature-dependent anisotropy indicates that scattering mechanism is different between in-plane and along c-axis, suggesting a quasi two-dimensional electronic structure.[16]

Figure 3 shows the temperature dependence of the Hall coefficient ( $R_H$ ) of the crystal.  $R_H$  is positive and shows strongly temperature dependent. Charge carrier concentration can be estimated from  $R_H$  at the room temperature to be  $1.33 \times 10^{21} \text{ cm}^{-3}$ , three times less than that observed in  $\text{Na}_{0.7}\text{CoO}_2$  [3] and two times larger than that observed in  $\text{Ca}_3\text{Co}_4\text{O}_9$ . [17] In the inset of Fig. 3, it is found that the high-temperature  $R_H$  is proportional to  $T^2$ , different from the linear temperature dependent  $R_H$  in  $\text{Na}_{0.7}\text{CoO}_2$ . [3] This suggests the different electronic structure between present misfit-layered cobaltite and  $\text{Na}_x\text{CoO}_2$ . Although  $\rho_{ab}$  is metallic down to 2 K, the  $R_H$  shows an upturn below about 70 K with decreasing temperature. Similar behavior in Hall coefficient has been observed in  $(\text{Bi,Pb})_2\text{Sr}_2\text{Co}_2\text{O}_y$  single crystals, [6] in which the upturn of  $R_H$  at low temperature is ascribed to anomalous Hall effect. However, the  $\rho_{xy}$  is linear to magnetic field down to 10 K in the present crystal, the anomalous Hall effect is not applicable here to interpret the upturn of  $R_H$ . The upturn of  $R_H$  may suggest either some localization of charge carrier at low temperature in spite of the metallic  $\rho_{ab}(T)$  down to 2 K or reduction of density of states at Fermi surface because of some unknown reasons.

Figure 4 shows the temperature dependence of the thermoelectric power (TEP). The value of TEP at room temperature is  $\approx +110 \mu\text{V}/\text{K}$ , as large as that in  $\text{Na}_{0.75}\text{CoO}_2$ . However,  $[\text{Bi}_2\text{Ba}_{1.3}\text{K}_{0.6}\text{Co}_{0.1}]^{RS}[\text{CoO}_2]_{1.97}$  has larger resistivity than that of  $\text{Na}_{0.75}\text{CoO}_2$ . [18] TEP decreases with decreasing temperature. The calculated power factor  $Q = S^2/\rho$  is  $3.2 \times 10^{-4} \text{ W m}^{-1} \text{ K}^{-2}$ , larger than those observed in  $\text{Bi}_2\text{Ca}_2\text{Co}_2\text{O}_y$  ( $\approx 2.7 \times 10^{-4} \text{ W m}^{-1} \text{ K}^{-2}$ ) and  $\text{Ca}_3\text{Co}_4\text{O}_9$  ( $\approx 1.8 \times 10^{-4} \text{ W m}^{-1} \text{ K}^{-2}$ ) single crystals. [19]  $Q$  increases to  $6.5 \times 10^{-4} \text{ W m}^{-1} \text{ K}^{-2}$  at around 100 K and then decreases with decreasing temperature. This maximum is much larger than those obtained maximum of  $Q$  in  $\text{Bi}_2\text{Ca}_2\text{Co}_2\text{O}_y$  ( $\approx 3.2 \times 10^{-4} \text{ W m}^{-1} \text{ K}^{-2}$ ) and  $\text{Ca}_3\text{Co}_4\text{O}_9$  ( $\approx 2.1 \times 10^{-4} \text{ W m}^{-1} \text{ K}^{-2}$ ) single crystals. [19] This indicates that  $[\text{Bi}_2\text{Ba}_{1.3}\text{K}_{0.6}\text{Co}_{0.1}]^{RS}[\text{CoO}_2]_{1.97}$  single crystal has a better thermoelectric performance than those in  $\text{Bi}_2\text{Ca}_2\text{Co}_2\text{O}_y$  and  $\text{Ca}_3\text{Co}_4\text{O}_9$  single crystals. [19] But the thermoelectric performance of  $[\text{Bi}_2\text{Ba}_{1.3}\text{K}_{0.6}\text{Co}_{0.1}]^{RS}[\text{CoO}_2]_{1.97}$  single crystal is lower than those observed in  $\text{Na}_x\text{CoO}_2$  ( $x \geq 0.70$ ) according to the data reported by Lee et al. [18]

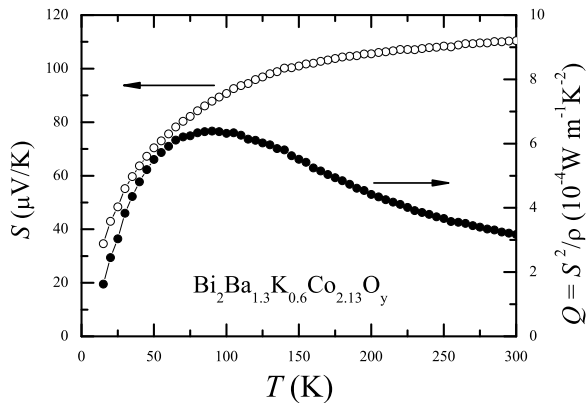


FIG. 4: Temperature dependence of thermoelectric power (TEP) and power factor for  $[\text{Bi}_2\text{Ba}_{1.3}\text{K}_{0.6}\text{Co}_{0.1}]^{\text{RS}}[\text{CoO}_2]_{1.97}$  single crystal.

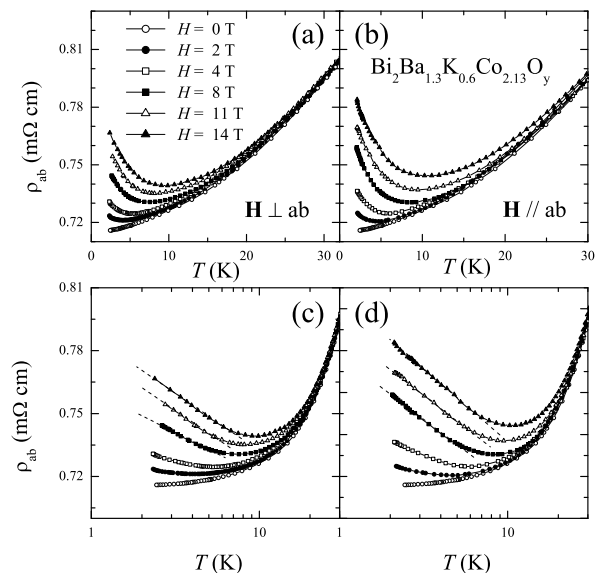


FIG. 5: Temperature dependence of in-plane magnetoresistivity under different magnetic field (a): perpendicular and (b): parallel to  $ab$  plane for the  $[\text{Bi}_2\text{Ba}_{1.3}\text{K}_{0.6}\text{Co}_{0.1}]^{\text{RS}}[\text{CoO}_2]_{1.97}$  single crystal. (c) and (d) are replotted of (a) and (b) in  $\log(T)$  scale, respectively. The dashed lines guide eyes linear to  $\ln(1/T)$ .

### C. Magnetotransport

Figure 5 shows the temperature dependence of in-plane resistivity under different magnetic fields ( $H$ ) varying from 0 to 14 T. Striking feature is observed that magnetic field leads to a transition from metallic to semiconductor-like behavior at low temperature with  $H$  either perpendicular or parallel to the  $ab$  plane. The minimum resis-

tivity appears in  $\rho_{ab}(T)$  and obvious positive magnetoresistance (MR) is observed. As shown in Fig.5, the temperature corresponding to the minimum resistivity shifts to high temperature with increasing magnetic field. At 2.5 K and 8 T, the positive MR reaches 4% as  $H$  lies in  $ab$  plane and 6% as  $H$  is along the  $c$ -axis, respectively. This value is much lower than that observed in undoped polycrystalline sample, where about 10% of MR was observed at 2.5 and 7 T.[12] The effect of  $H$  on  $\rho_{ab}(T)$  is stronger with  $H//ab$  plane than that with  $H \perp ab$  plane. As shown in Fig.6, similar effect of  $H$  on  $\rho_c(T)$  is also observed. Although the upturn of  $\rho_c(T)$  at low temperature follows a thermal activation behavior without magnetic field, external magnetic field leads to a change of low temperature resistivity from a thermal activation behavior to a  $\ln(1/T)$  diverging behavior with  $H$  either perpendicular or parallel to the  $ab$  plane. It suggests that  $\rho_{ab}(T)$  and  $\rho_c(T)$  show the same temperature dependence under  $H$  at low temperature although they show contrasting behavior (metallic in  $\rho_{ab}(T)$  and semiconducting in  $\rho_c(T)$ ) without  $H$ .

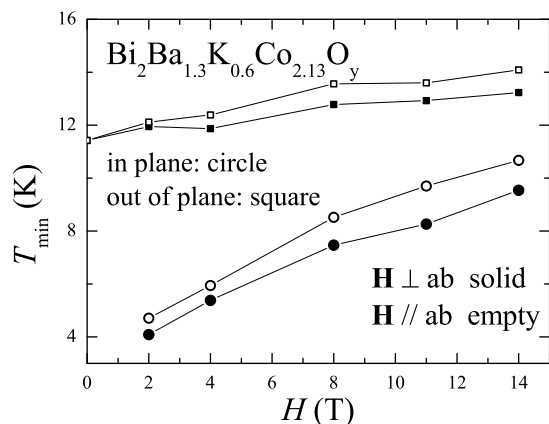


FIG. 6: Temperature dependence of out-of-plane magnetoresistivity under different magnetic field (a): perpendicular and (b): parallel to  $ab$  plane for the  $[\text{Bi}_2\text{Ba}_{1.3}\text{K}_{0.6}\text{Co}_{0.1}]^{\text{RS}}[\text{CoO}_2]_{1.97}$  single crystal.

Figure 7 shows the magnetic field dependence of the temperature corresponding to the minimum resistivity ( $\rho_{ab}(T)$  and  $\rho_c(T)$ ). It indicates that the temperature corresponding to the minimum resistivity ( $T_{min}$ ) increases with increasing  $H$ , suggesting that the localization is enhanced by  $H$ . It should be pointed out that  $T_{min}$  in  $\rho_c(T)$  is enhanced slightly with increasing magnetic field, contrasting to the strong dependence of  $T_{min}$  in  $\rho_{ab}(T)$ . Negative MR is a common feature in  $\text{Ca}_3\text{Co}_4\text{O}_9$  and  $(\text{Bi,Pb})_2\text{M}_2\text{Co}_2\text{O}_y$  ( $M = \text{Sr}$  and  $\text{Ca}$ ), in which semiconducting resistivity can usually be observed below a certain temperature.[2, 6, 7] While with  $M = \text{Ba}$ , large positive MR has been observed in polycrystalline

sample.[12] The negative MR has been explained to be related to the spin-dependent transport at temperatures below or close to the magnetic ordering transitions, while the positive MR is not clearly understood. In the previous reports, no such obvious positive MR has been found in a *metallic* triangular cobaltites: either  $\text{Ti}_{0.4}\text{SrCoO}_x$  or  $\text{Na}_x\text{CoO}_2$ .  $\text{Na}_{0.75}\text{CoO}_2$  is exceptional case, spin density wave (SDW) has been taken into account for interpreting the anomalously large positive MR in it.[20] We tried to fit the  $\rho_{ab}(T)$  at  $H=8, 11$  and  $14$  T below  $T_{min}$  with a variety of functional forms. It turned out that the resistivity at low temperature under  $H$  cannot be fitted by the formula including thermal activation ( $\ln\rho \sim -1/T$ ), various types of variable range hopping (VRH) conduction ( $\ln\rho \sim -T^{-\alpha}$  with  $\alpha=\frac{1}{2}, \frac{1}{3}$  and  $\frac{1}{4}$ ) and power law ( $\ln\rho \sim \ln T$ ). Instead, the data at high magnetic field with  $H$  either perpendicular or parallel to the  $ab$  plane exhibit a  $\ln(1/T)$  divergence [ $\rho \sim \ln(1/T)$ ] as shown in Fig.5c, 5d and Fig.6. Such magnetic-field-induced localization has not been observed yet in the triangular layered cobaltites previously.

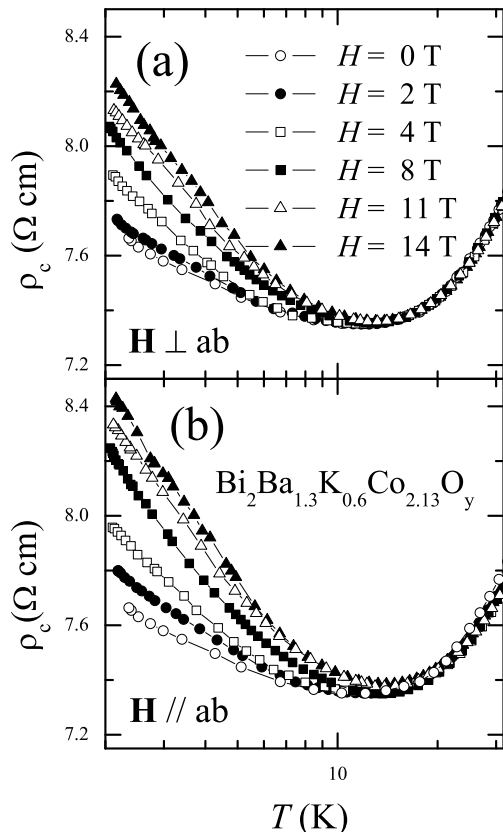


FIG. 7: The temperature corresponding to the minimum  $\rho_{ab}(T)$  and  $\rho_c(T)$  as a function of magnetic field with  $H$  parallel and perpendicular to  $ab$  plane for the  $[\text{Bi}_2\text{Ba}_{1.3}\text{K}_{0.6}\text{Co}_{0.1}]^{RS}[\text{CoO}_2]_{1.97}$  single crystal.

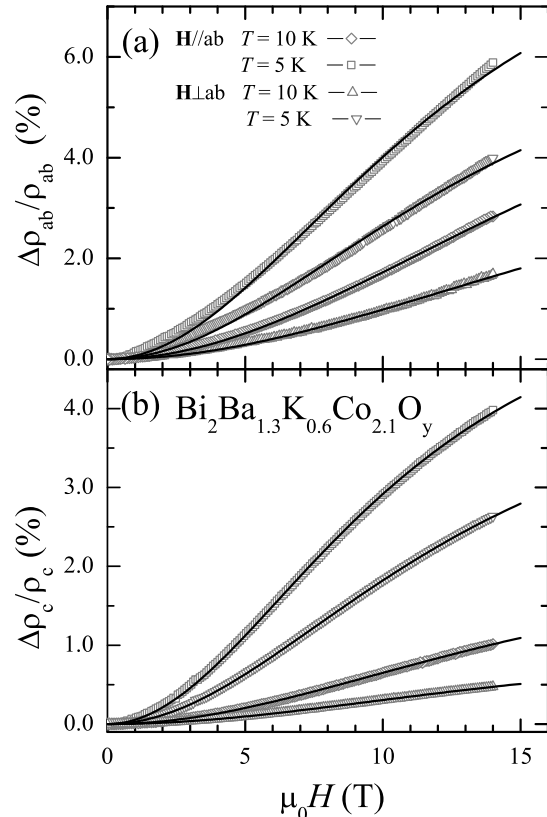


FIG. 8: Magnetic-field dependence of the in-plane and out-of-plane isothermal MR with  $H$  parallel and perpendicular to  $ab$  plane for the  $[\text{Bi}_2\text{Ba}_{1.3}\text{K}_{0.6}\text{Co}_{0.1}]^{RS}[\text{CoO}_2]_{1.97}$  single crystal. The solid lines are the fitting results with Eqn.(1).

The in-plane and out-of-plane isothermal MRs were measured at 5 K and 10 K with  $H$  varying from 0 to 14 T as shown in Fig. 8. All the MRs are positive and increase with lowering temperature. The value of MR with  $H//ab$  is larger than that with  $H//c$  at a fixed temperature. The MR does not follow the classical  $H^2$  law or Kohler's law (i.e. collapsing to a single curve in Kohler plot,  $\delta\rho/\rho$  vs.  $H/\rho_0$ ). The MRs do not follow a linear relationship to  $H$ , as claimed by Hervieu et al. in undoped polycrystalline sample.[12] These unusual positive MRs may be related to the magnetic-field-induced localization as indicated in Fig.5 and Fig.6.

#### IV. DISCUSSIONS AND CONCLUSIONS

Magnetotransport behavior can usually be related to the Fermi surface.[21] For example, a square Fermi surface can lead to a linear MR due to the presence of a sharp corners.[21] For systems with multiband electronic structure involving two types of charge carriers, the  $H$

dependence of MR can be written as

$$\Delta\rho/\rho(0) = aH^2/(b + cH^2) \quad (1)$$

where  $a$ ,  $b$  and  $c$  are positive,  $H$ -independent quantities determined by the relaxation rates of each type of charge carrier.[22] Local density approximation (LDA) calculations in  $\text{NaCo}_2\text{O}_4$  predicted a large cylindrical Fermi surface around  $\Gamma$ - $A$  line, surrounding by small satellite hole-like pockets centered about 2/3 of the way out on the  $\Gamma$ - $K$  and  $A$ - $H$  directions.[23] In  $\text{Na}_x\text{CoO}_2$ , however, no such satellite hole-like pocket has been experimentally observed.[24] Interestingly, Feng et al. found that the square  $\text{BiO}$  layer is also conducting except for the triangle  $\text{Co-O}$  layer in the same  $[\text{Bi}_2\text{Ba}_{1.3}\text{K}_{0.6}\text{Co}_{0.1}]^{\text{RS}}[\text{CoO}_2]_{1.97}$  single crystal through ARPES.[25] The electronic structure of  $[\text{Bi}_2\text{Ba}_{1.3}\text{K}_{0.6}\text{Co}_{0.1}]^{\text{RS}}[\text{CoO}_2]_{1.97}$  is different from that of  $\text{Na}_x\text{CoO}_2$ . Therefore, multiband electronic structure does exist in  $[\text{Bi}_2\text{Ba}_{1.3}\text{K}_{0.6}\text{Co}_{0.1}]^{\text{RS}}[\text{CoO}_2]_{1.97}$  single crystal. Furthermore, because of the peculiar rhombohedral coordination the  $t_{2g}$  orbitals of the low-spin  $\text{Co}^{3+}$  and  $\text{Co}^{4+}$  in the triangular cobaltites would be split, forming heavy  $a_{1g}$  and light  $e'_g$  holes.[23, 26] Consequently, we tried to fit the MR data shown in Fig.8 using Eqn.(1). Surprisingly, the out-of-plane MR data can be well fitted using Eqn.(1) as shown in Fig.8. The in-plane MR data can also be roughly fitted. Therefore, it suggests that the positive MR in this crystal possibly results from the multiband electronic structure with two types of charge carriers.

Slight deviation from Eqn.(1) is observed for the in-plane isothermal MRs. Therefore, there could be some other mechanisms for this positive MR in addition to the multiband electronic structure. A magnetic-field-induced logarithmic temperature dependence of in-plane resistivity has been observed as shown in Fig. 5c and 5d. Such magnetic-field-induced logarithmic temperature-dependent resistivity has been reported in high- $T_c$  cuprates, in which the logarithmically temperature-dependent resistivity appears when superconductivity is suppressed by external magnetic field.[27] There are two main points of view to interpret such logarithmic resistivity. In cuprates, *field-induced* SDW state has been taken as one of the points of view to interpret the logarithmically temperature-dependent resistivity.[28, 29, 30] In most misfit-layered triangular cobaltites, such as  $\text{Ca}_3\text{Co}_4\text{O}_9$ ,  $(\text{Bi,Pb})_2\text{M}_2\text{Co}_2\text{O}_y$  ( $M=\text{Ca}$  and  $\text{Sr}$ ), SDW is a common spin ordered state.[10] Determining from the  $\mu\text{SR}$  results, however, no SDW exists down to 1.8 K at zero or low field in updoped  $\text{Bi}_2\text{Ba}_2\text{Co}_2\text{O}_y$ ,[10] with large positive MR at low temperature. It could be believed that  $[\text{Bi}_2\text{Ba}_{1.3}\text{K}_{0.6}\text{Co}_{0.1}]^{\text{RS}}[\text{CoO}_2]_{1.97}$  single crystal have no SDW state because of the much better metal-

licity compared to the updoped  $\text{Bi}_2\text{Ba}_2\text{Co}_2\text{O}_y$  sample. If the logarithmically temperature-dependent resistivity in  $[\text{Bi}_2\text{Ba}_{1.3}\text{K}_{0.6}\text{Co}_{0.1}]^{\text{RS}}[\text{CoO}_2]_{1.97}$  single crystal arise from the SDW order as that in high- $T_c$  cuprates, the SDW state should be field-induced. Up to now, however, no evidence for the field-induced SDW has been reported. Consequently,  $\mu\text{SR}$  experiments in high magnetic field could be desired to turn out whether the SDW can be induced in the present compound by magnetic field.

Another point of view is the weak localization in 2D systems,[31, 32] which theoretically predicts a logarithmic temperature dependence of the conductivity.[33] The misfit structure leads to the system to be 2-dimensional structurally. The large anisotropy and the strong temperature dependence of the anisotropy as shown in Fig.2 suggests the  $[\text{Bi}_2\text{Ba}_{1.3}\text{K}_{0.6}\text{Co}_{0.1}]^{\text{RS}}[\text{CoO}_2]_{1.97}$  single crystal to be a (quasi) 2D electronic system. Evidencing from these results, it is also possible that field-induced 2D weak localization results in the logarithmically temperature-dependent resistivity. This is reason why the in-plane MR data are roughly fitted with slight deviation based on the multiband electronic structure with two types of charge carriers.

In conclusion, resistivity under magnetic field, thermopower and Hall coefficient are systematically studied for  $[\text{Bi}_2\text{Ba}_{1.3}\text{K}_{0.6}\text{Co}_{0.1}]^{\text{RS}}[\text{CoO}_2]_{1.97}$  single crystal. An anomalous behavior is observed that there exist a contrasting behavior at low temperature in in-plane resistivity ( $\rho_{ab}(T)$ ) and out-of-plane ( $\rho_c(T)$ ): metallic behavior down to 2 K with a  $T^2$  dependence below 30 K in  $\rho_{ab}(T)$ ; while a thermal activation semiconducting behavior below about 12 K in  $\rho_c(T)$ . Magnetic field leads to a  $\ln(1/T)$  diverging behavior in both  $\rho_{ab}$  and  $\rho_c(T)$  at low temperature. The isothermal out-of-plane MR can be quite well fitted by taking into account the multiband electronic structure with two types of charge carriers. The  $\ln(1/T)$  diverging  $\rho_{ab}(T)$  in magnetic field could arise from the field-induced 2D weak localization or magnetic field induced spin density wave.

## V. ACKNOWLEDGEMENT

This work is supported by the National Natural Science Foundation of China and by the Ministry of Science and Technology of China (973 project No: 2006CB601001 and 2006CB0L1205).

\* Corresponding author. *Electronic address:* chenxh@ustc.edu.cn

[1] I. Terasaki, Y. Sasago, and K. Uchinokura, Phys. Rev. B **56**, R12685 (1997).

[2] A. C. Masset, C. Michel, A. Maignan, M. Hervieu, O. Toulemonde, F. Studer, and B. Raveau, Phys. Rev. B

- 62**, 166 (2000).
- [3] Y. Y. Wang, N. S. Rogado, R. J. Cava, and N. P. Ong, (London) **423**, 425(2003); Y. Y. Wang, N. S. Rogado, R. J. Cava, and N. P. Ong, cond-mat/0305455.
- [4] S. Y. Li, L. Taillefer, D. G. Hawthorn, M. A. Tanatar, J. Paglione, M. Sutherland, R. W. Hill, C. H. Wang, and X. H. Chen, Phys. Rev. Lett. **93**, 056401 (2004).
- [5] K. Takada, H. Sakurai, E. Takayama-Muromachi, F. Izumi, R. A. Dilanian, and T. Sasaki, Nature **422**, 53 (2003).
- [6] T. Yamamoto, I. Tsukada, M. Takagi, T. Tsubone, and K. Uchinokura, J. Magn. Magn. Mater. **226-230**, 2031 (2001); T. Yamamoto, K. Uchinokura, and I. Tsukada, Phys. Rev. B **65**, 184434 (2002).
- [7] A. Maignan, S. Hebert, M. Hervieu, C. Machel, D. Pelloquin and D. Khomskii, J. Phys: Condens. Matter **15**, 2711 (2003).
- [8] M. L. Foo, Y. Y. Wang, S. Watauchi, H. W. Zandbergen, T. He, R.J. Cava, and N.P. Ong, Phys. Rev. Lett. **92**, 247001 (2004).
- [9] C. H. Wang, X. H. Chen, T. Wu, X. G. Luo, G. Y. Wang, and J. L. Luo Phys. Rev. Lett. **96**, 216401(2006).
- [10] J. Sugiyama, J. H. Brewer, E. J. Ansaldo, H. Itahara, T. Tani, M. Mikami, Y. Mori, T. Sasaki, S. Hebert, and A. Maignan, Phys. Rev. Lett. **92**, 017602 (2004).
- [11] H. Leligny, D. Grebille, O. Perez, A. C. Masset, M. Hervieu, C. Michel, and B. Raveau, C. R. Sci. Paris IIc, Chim **2**, 409 (1999); Acta Crystallogr., Sect. B: Struct. Sci. **56**, 173 (2000).
- [12] M. Hervieu, A. Maignan, C. Michel, V. Hardy, N. Creon, and B. Raveau, Phys. Rev. B **67**, 045112 (2003).
- [13] X. G. Luo, X. H. Chen, G. Y. Wang, C. H. Wang, X. Li, W. J. Miao, G. Wu, and Y. M. Xiong, Eur. Phys. J. B. **49**,37 (2006).
- [14] R. D. Shannon, Acta Crystallogr. **A32**, 751 (1976); R. D. Shannon, C. T. Prewitt, Acta Crystallogr. **B25**, 925 (1969).
- [15] T. Valla, P. D. Johnson, Z. Yusof, B. Wells, Q. Li, S. M. Loureiro, R. J. Cava, M. Mikami, Y. Mori, M. Yoshimura, and T. Sasaki, Nature **417**, 627 (2002); Z. Yusof, B.O. Wells, T. Valla, P.D. Johnson, A.V. Fedorov, Q. Li, S.M. Loureiro, R.J. Cava, cond-mat/0610271.
- [16] X. H. Chen, M. Yu, K. Q. Ruan, S. Y. Li, Z. Gui, G. C. Zhang, and L. Z. Cao, Phys. Rev. B **58**, 14219(1998).
- [17] X. G. Luo, X. H. Chen, C. H. Wang, G. Y. Wang, Y. M. Xiong, H. B. Song, H. Li, and X. X. Lu Europhys. Lett. **74**, 526 (2006).
- [18] M. Lee, L. Viciu, Lu Li, Y. Y. Wang, M. L. Foo, S. Watauchi, R. A. Pascal Jr., R. J. Cava, and N. P. Ong, Nature Materials **425**, 537 (2006).
- [19] X. G. Luo, Y. C. Jing, H. Chen, and X. H. Chen, J. Cryst. Growth, in press.
- [20] T. Motohashi, R. Ueda, E. Naujalis, T. Tojo, I. Terasaki, T. Atake, M. Karppinen, and H. Yamauchi, Phys. Rev. B **67**, 064406 (2003).
- [21] A. B. Pippard, *Magnetoresistance in Metal* (Cambridge University Press, Cambridge, 1989).
- [22] J. M. Ziman, *Principles of the Theory of Solids*, 2nd ed. (Cambridge University Press, Cambridge, 1972).
- [23] D. J. Singh, Phys. Rev. B **61**, 13397 (2000).
- [24] M. Z. Hasan, Y. D. Chuang, D. Qian, Y.W. Li, Y. Kong, A. Kuprin, A.V. Fedorov, R. Kimmerling, E. Rotenberg, K. Rossnagel, Z. Hussain, H. Koh, N.S. Rogado, M.L. Foo, and R.J. Cava, Phys. Rev. Lett. **92**, 246402 (2004).
- [25] D. L. Feng, private communication.
- [26] T. Mizokawa, L. H. Tjung, P. G. Steeneker, N. B. Brookes, I.Tsukada, T. Yamamoto, and K. Uchinokura, Phys. Rev. B **64**, 115104 (2001).
- [27] Y. Ando, G. S. Boebinger, A. Passner, T. Kimura, and K. Kishio, Phys. Rev. Lett. **75**, 4662 (1995).
- [28] X. F. Sun, S. Komiya, J. Takeya, and Y. Ando, Phys. Rev. Lett. **90** 117004 (2003).
- [29] S. Komiya and Y. Ando, Phys. Rev. B **70** 060503 (2004).
- [30] X. G. Luo, X. H. Chen, X. Liu, R. T. Wang, C. H. Wang, L. Huang, L. Wang, and Y. M. Xiong, Supercond. Sci. & Technol. **18** 234 (2005).
- [31] Y. Hidaka, Y. Yamaji, K. Sugiyama, F. Tomiyama, A. Yamagishi, M. Date, M. Hikita, J. Phys. Soc. Jpn. **60**, 1185 (1991).
- [32] S. J. Hagen, X. Q. Xu, W. Jiang, J. L. Peng, Z. Y. Li and R. L. Greene, Phys. Rev. B **45**, 515 (1992).
- [33] G. Bergmann, Phys. Reports **107**, 1 (1984).